Diffusive dynamics and jamming in ensembles of robots with variable friction

Diffusive dynamics and jamming in ensembles of robots with variable friction

A D Rozenblit[1,2], V A Porvatov[3,4], D A Petrova[3,4], I S Khakhalin[5], K P Kotlyar[6], G Yu Gritsenko[7], A A Evreiskaya[8], M F Lebedeva[6], E I Kretov[9], D S Filonov[4], A Souslov[10], and N A Olekhno[1*]

[1]ITMO University, 197101 Saint Petersburg, Russia
[2]Peter the Great St. Petersburg Polytechnic University, 195251 Saint Petersburg, Russia
[3]National University of Science and Technology "MISIS", 119991 Moscow, Russia
[4]Moscow Institute of Physics and Technology, 141701 Moscow, Russia
[5]Baltic State Technical University 190005, Saint Petersburg, Russia
[6]Alferov University, 194021 Saint Petersburg, Russia
[7]Lomonosov Moscow State University, 119991 Moscow, Russia
[8]Novosibirsk State University, 630090 Novosibirsk, Russia
[9]Max Delbrück Center for Molecular Medicine in the Helmholtz Association, 13125 Berlin, Germany
[10]University of Bath, Bath, UK

E-mail: *olekhnon@gmail.com

Abstract. In the present paper, we experimentally study the diffusive dynamics in ensembles of self-propelled and self-rotating bristle-bots. Considering the dependence of the system dynamics on the packing density of robots as well as on the friction between individual robots, we show that the friction slightly affects the diffusive dynamics but leads to a significant change in the jamming transition corresponding to the formation of rigid clusters of robots.

1. Introduction

Physics of active matter considers the dynamics of systems composed of particles that can extract energy from their sources and convert this energy into individual and collective motion. Examples of such systems include biological ones such as bacterial colonies [1], flocks of birds or fish [2], as well as artificial systems, including ensembles of self-propelled micro-particles [3] or macroscopic robots [4, 5, 6]. The latter platform is especially attractive for experimental studies due to its low cost and great flexibility which allows engineering properties of individual particles. Various phenomena have also been studied in ensembles of self-rotating particles, including phase separation [7] and mixing [8] of particles rotating clockwise and counterclockwise, reversal of collective rotation of active spinners having the same chirality depending on their packing density [9], theory of jamming and unjamming of active rotators [10], and dynamics of active spinners embedded in passive media [11]. However, the dependence of collective behavior of self-propelled or self-rotating robots on friction between individual robots have not been studied in detail. In the present paper, we focus on diffusive dynamics and jamming transition in such active ensembles.

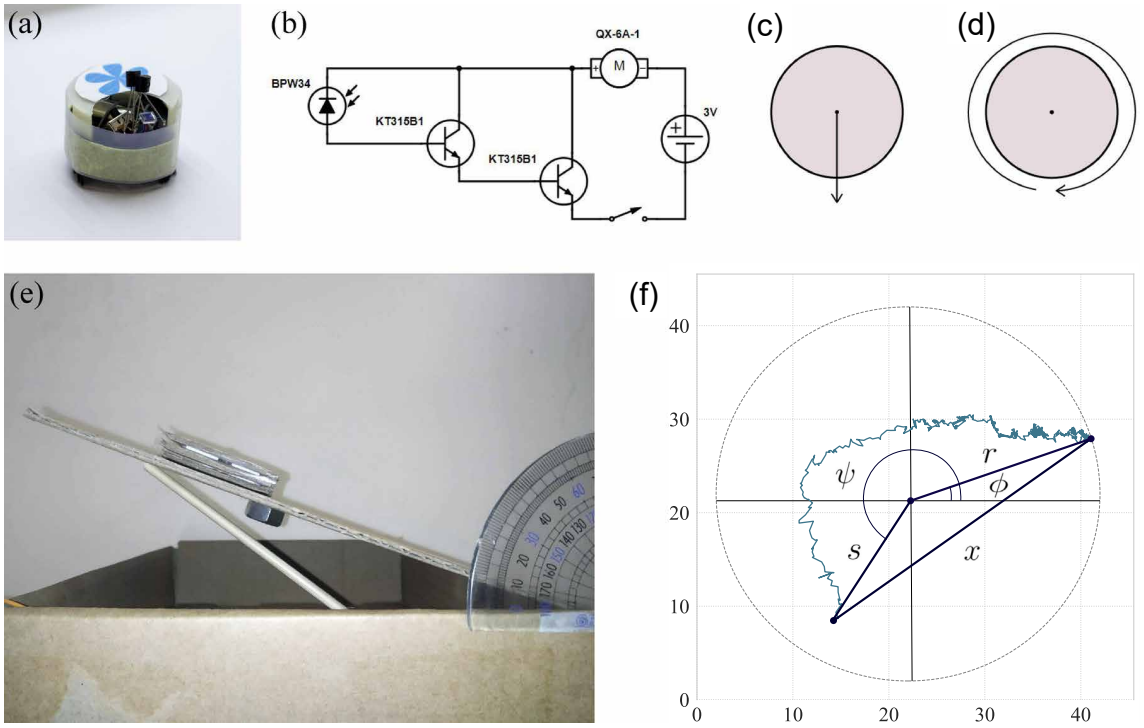

Figure 1. Experimental setup. (a): Photograph of the self-propelled bristle bot used in the experimental setup. (b): Schematics of the robot control circuit which includes a power source, a photodiode, two transistors and a vibration motor. (c, d): Schematic representation of the self-propelled (c) and self-rotating (d) robots movement patterns. (e): Setup for the measurement of static friction coefficients. (f): Displacement between the given initial location of moving particle and the position of collision with the boundary for some arbitrary trajectory of the particle.

2. Experimental setup

In the present work, we consider the ensembles of 33 self-propelled and 22 self-rotating bristle-bots (10 clockwise and 12 counterclockwise) vibrating at frequencies between 50 and 100 Hz, figure 1a. The vibration causes bristle-bots having soft deformable legs to move due to the asymmetry of their shape and mass distribution. Each robot is 35 mm in diameter and consists of the body made of ABS plastic via FDM printing technology, QX-6A-1 vibration motor, a 3V battery, and a control circuit. The circuit allows turning the robots on and off by changing the ambient lighting and includes two KT315B1 transistors, Vishay BPW34 PIN photodiode and KLS7-SS03-12D02 slide switch, figure 1b. The robots are placed inside the plastic boundary of a variable diameter that is changed between 20 and 40 cm to control the density of robots. To change the friction between robots, side surfaces of individual bristle-bots are covered with different materials ranging from a sandpaper to a paper tape to a plastic tape. The motion of the system is captured with a camera and then analyzed with the aid of DeepLabCut neural network and OpenCV Library.

To obtain numerical values of friction coefficients for the used materials, we measure the static friction coefficient k of the plastic tape, paper tape and sandpaper directly as the tangent of the angle at which the test body covered with a given material starts to slide on the inclined plane covered with the same material, figure 1e. The inclination angle is controlled and measured by the setup including servo motor Tower Pro SG90, potentiometer S16KN1-

B2K, and microcontroller ATMega2560. The results are averaged over three measurements. The obtained static friction coefficient values are $k_{\text{low}} = 0.26$, $k_{\text{med}} = 0.40$, and $k_{\text{high}} = 0.96$ for the plastic tape, paper tape, and sandpaper, respectively.

3. Dynamics of self-propelled particles

We consider the dependence of the dynamics of robotic ensemble on the robot density p and friction coefficient between individual robots k. To do so, we extract trajectories of individual robots for different diameters of the boundary D and different materials covering robots. Then, we study a root mean square displacement of robots as a function of time, averaged over N different trajectories in the single realization as well as over three different initial configurations of the ensemble:

$$x(t) = \frac{1}{3N} \sum_{i=1}^{3N} \sqrt{(x_0^{(i)} - x_1^{(i)}(t))^2 + (y_0^{(i)} - y_1^{(i)}(t))^2}, \tag{1}$$

where $(x_0^{(i)}, y_0^{(i)})$ is the initial position of the particle corresponding to the i^{th} trajectory, and $(x_1^{(i)}(t), y_1^{(i)}(t))$ is the position of the same particle at the moment t. In the following, it is useful to compare the measured particle displacements with some estimation value of typical mean displacement of the particle initially located at a random position within the considered system and the boundary. Such a quantity is given by the integral

$$M = \frac{\int_0^r \int_0^{2\pi} \int_0^{2\pi} x(s, \phi, \psi) ds d\varphi d\psi}{\int_0^r ds \int_0^{2\pi} d\varphi \int_0^{2\pi} d\psi}, \tag{2}$$

where

$$x(s, \phi, \psi) = \sqrt{r^2 + s^2 - 2rs\cos(\phi - \psi)}, \tag{3}$$

as illustrated by the schematics shown in figure 1f. Numerical evaluation of this integral gives

$$M = 0.544D, \tag{4}$$

where D is the boundary diameter.

Another useful estimation is calculated as the maximum displacement of the particle until it reaches the boundary:

$$M_{\max} = \frac{\int_0^r \int_0^{2\pi} (r + s) ds d\varphi}{\int_0^r ds \int_0^{2\pi} d\varphi}. \tag{5}$$

Analytical evaluation of this integral gives

$$M_{\max} = 0.75D. \tag{6}$$

The first series of experiments are performed in the system consisting of 32 to 33 self-propelled bristle-bots. The bots of this type are characterized by a unidirectional motion, figure 1c. For each value of the friction coefficient and boundary diameters of $D = 30$, 33.5 and 40 cm, we studied three independent realizations of the system. Corresponding filling densities of the system read $p_1 = 0.35$, $p_2 = 0.25$, and $p_3 = 0.2$. Photographs of the system for different boundary diameters are shown in figure 2a-c. To analyze the captured robot trajectories, we applied the DeepLabCut neural network. The processed trajectories are shown in figure 2d-f.

Next, we analyze the time dependence of the root mean square displacement $x(t)$ for each robot in the log-log scale. All the curves shown in figure 2g-i are averaged over 5 to 6 marked robots, as well as over three independent realizations of the system corresponding to different

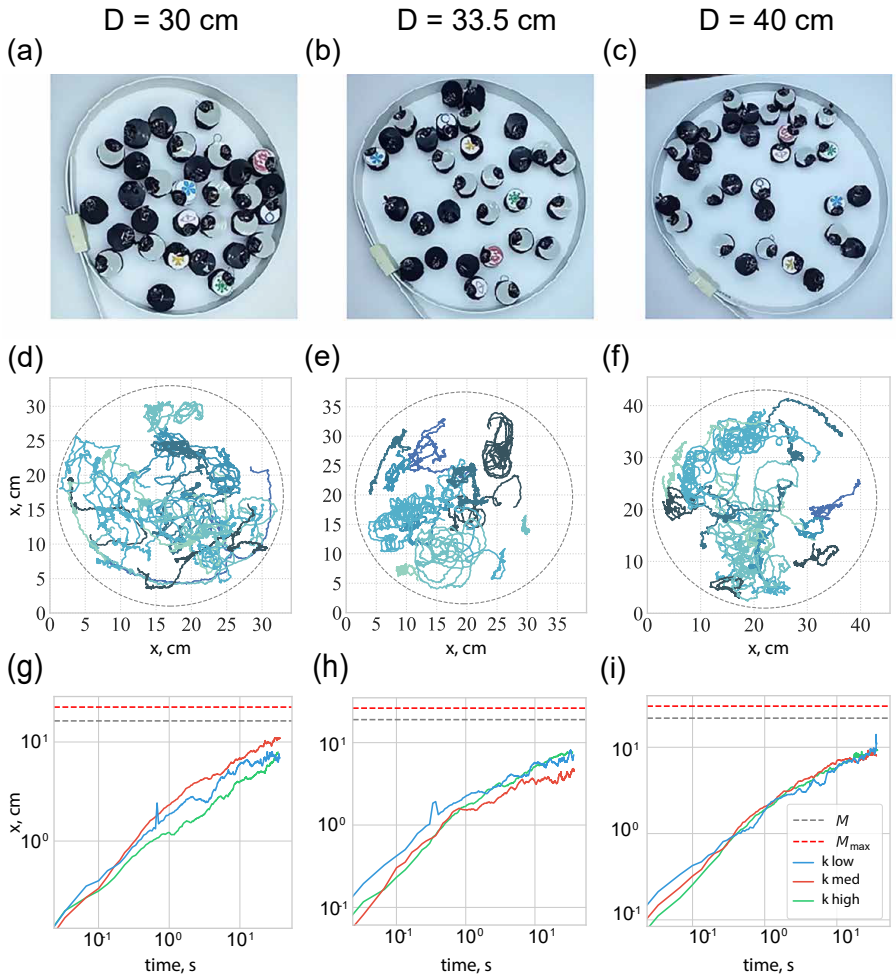

Figure 2. Experimental study of self-propelled particles. (a)-(c): Photographs of the system for various boundary diameters D. (d)-(f): Extracted trajectories of robots for particular realizations of systems corresponding to the same boundary diameters D as in panels (a)-(c). (g)-(i): Root mean square displacements of robots as a function of time $x(t)$ for different friction coefficients between robots $k_{\text{low}} = 0.26$ (blue solid line), $k_{\text{med}} = 0.4$ (red solid line), and $k_{\text{high}} = 0.96$ (green solid line). Grey and red dashed lines show estimations of the characteristic particle displacements M and M_{max}, correspondingly.

initial positions of the robots for each boundary diameter and friction value. From the plots shown in figure 2g-i, one can see the region corresponding to a ballistic motion

$$x(t) \propto t, \tag{7}$$

the region corresponding to the diffusive dynamics

$$x(t) \propto t^{\alpha}, \tag{8}$$

with a power law exponent $\alpha \approx 0.5$, and the plateau

$$x(t) = \text{const}, \tag{9}$$

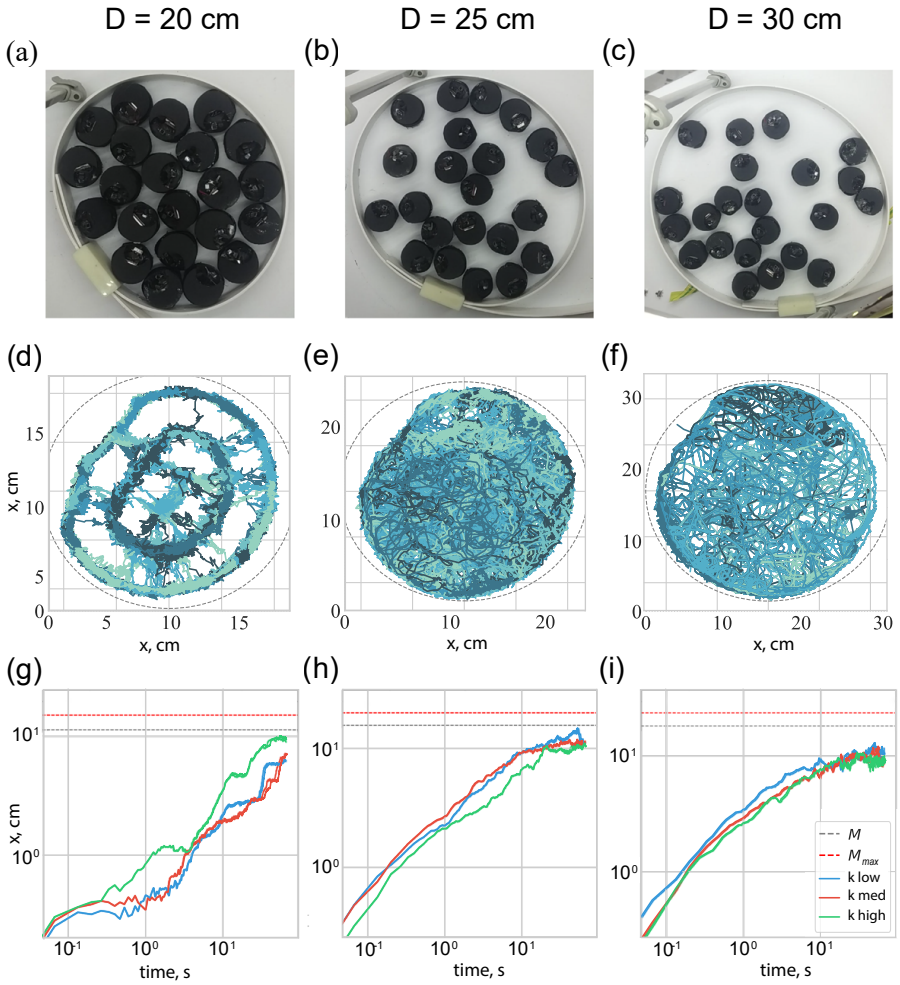

Figure 3. Experimental study of self-rotating particles. (a)-(c): Photographs of the system for various boundary diameters D. (d)-(f): Extracted trajectories of robots for particular realizations of systems corresponding to the same boundary diameters D as in panels (a)-(c). (g)-(i): Root mean square displacements of robots as a function of time $x(t)$ for different friction coefficients between robots $k_{\text{low}} = 0.26$ (blue solid line), $k_{\text{med}} = 0.4$ (red solid line), and $k_{\text{high}} = 0.96$ (green solid line). Grey and red dashed lines show estimations of the characteristic particle displacements M and M_{max}, correspondingly.

corresponding to the formation of a rigid cluster of robots, qualitatively resembling a glass. In the last case, the root mean square displacements of the robots practically do not change, even though the limiting maximal displacements M and M_{max} associated with the finite boundary diameter have not been reached. Since packing density of the system for all values of D shown in figure 2 is relatively low and is far from the bulk jamming transition point, this condensation of robots corresponds to the boundary-assisted jamming. It is seen that the diffusive motion weakly depends on friction since the slope of the curves corresponding to the region defined by Eq.(8) for all cases in figure 2g-i is practically the same. However, friction significantly affects the density at which jamming emerges. For example, in the figure 2h, jamming is more pronounced at the intermediate value of friction k_{med} than at high or low friction values. The obtained results demonstrate the possibility of a non-monotonic dependence of the jamming transition in active systems on friction between individual particles.

4. Dynamics of self-rotating particles

In the second series of experiments, we studied the system of 22 self-rotating particles, which are bristle-bots actively rotating around their axis with nearly no translational displacement, figure 1d. The same materials as in the first setup were used to obtain different friction between robots. Field diameters are $D = 20$, 25 and 30 cm, and corresponding filling densities of the system are $p_1 = 0.56$, $p_2 = 0.36$, and $p_3 = 0.25$, figure 3a-c. To analyze captured videos and extract trajectories of individual robots shown in figure 3d-f, Hough transform from the OpenCV Library is applied. The results are averaged over 18 to 22 bristle-bots in each implementation of the system, as well as over three independent realizations corresponding to different initial positions of the robots. There is a small difference in the number of statistical samples for different realizations, as in the previous setup, because not all robots were successfully recognized.

The dependencies of the root mean square displacement on time $x(t)$ shown in figure 3g-i demonstrate that at lower densities robots move diffusively, while at high densities there are multiple jamming transitions, which correspond to plateaus in the $x(t)$ curves. As seen in figure 3g, at high densities larger robot mobility is observed at the highest friction between robots, in contrast to low system fillings, and that at low friction jamming and release of robots goes faster. This highlights the role of friction in mechanisms leading to the conversion of robot rotation into motion as well as in the formation of stable clusters.

5. Conclusion

We experimentally studied the behavior of the active system of robots at different filling densities of the system, as well as at different values of the friction coefficient between robots. Two different systems were considered: self-propelled particles and self-rotating particles. Experiments with ensembles of self-propelled particles show that the boundary-assisted jamming transition corresponding to the formation of an active glass of robots significantly depends on friction between the robots, while the diffusive dynamics corresponding to the liquid-like behavior of the active system remains unchanged. Experiments with ensembles of self-rotating particles demonstrate that multiple jamming transitions can be observed at high densities of the system, and emphasize the possibility of a non-monotonic dependence of the mobility of robots on the friction between them.

Acknowledgments

We acknowledge fruitful discussions with Alexander Poddubny, Maxim Gorlach and Alexey Slobozhanyuk. The research was partly done during the Winter School at Alferov University, Saint Petersburg, Russia, and is partially supported by ITMO University and Alferov University.

References

[1] Mathijssen A J T M, Guzmán-Lastra F, Kaiser A, and Löwen H 2018 *Phys. Rev. Lett.* **121** 248101
[2] Filella A, Nadal F, Sire C, Kanso E, and Eloy C 2018 *Phys. Rev. Lett.* **120** 198101
[3] Bricard A, Caussin J-B, Desreumaux N, Dauchot O, and Bartolo D 2013 *Nature* **503** 95-98
[4] Giomi L, Hawley-Weld N, and Mahadevan L 2012 *Proc. R. Soc. A* **469** 20120637
[5] Slavkov I et al 2018 *Sci. Robot.* **3** eaau9178
[6] Deblais A, Barois T, Guerin T, Delville P H, Vaudaine R 2018 *Phys. Rev. Lett.* **120** 188002
[7] Scholz C, Engel M, and P oschel T 2018 *Nat. Commun.* **9** 931
[8] Ai B-Q, Shao Z-G, and Zhong W-R 2018 *Soft Matter* **14** 4388-4395
[9] Workamp M et al 2018 *Soft Matter* **14** 5572-5580
[10] Ravazzano L et al 2020 *Soft Matter* **16** 5478-5486
[11] Aragones J L, Steimal J P, and Alexander-Katz A 2019 *Soft Matter* **15** 3929-3937